CHAPTER V
MOLECULAR SIZE ESTIMATION AS AN EVIDENCE ON REMOVAL OF AROMATIC AND SULFUR COMPOUNDS IN TIRE-DERIVED OIL USING MESOPOROUS Al-MCM-41 AND Al-SBA-15 WITH DIFFERENT PORE SIZES

5.1 Abstract

In the fact that the aromatic compounds (MAHs, DAHs, PAHs, and PPAHs) are mainly present in tire-derived oil and mostly distributed in gas oil and vacuum gas oil fractions, they can cause the environmental and vehicle engine problems if tire-derived oil is directly used. Therefore, they need to be removed. In this work, the commercial Al-MCM-41 (pore size = 33.1 Å) and Al-SBA-15 (pore size = 60.5 Å) with the similar hexagonal structure and acid density were thus acquired. The effects of pore size on removal of large and heavy aromatics and sulfur compounds from oil were investigated. Estimation of average sizes of molecules in tire-derived oils was also carried out in order to investigate the hydrocarbon groups mostly affected by the mesoporous catalysts with different pore sizes. The catalytic pyrolysis of waste tire was operated in a batch reactor. GC×GC-TOF/MS and SIMDIST-GC instruments were used to analyze the liquid products for their chemical compositions and petroleum fraction, respectively. Furthermore, hetero-atoms (sulfur and nitrogen) in the pyrolysis products were determined using CHNS-analyzer. As a result, both mesoporous catalysts with the pore sizes of 33.1 and 60.5 Å can provide the almost complete cracking of large-size poly- and polar-aromatics in tire-derived oil. However, Al-MCM-41 with more suitable pore size of 33.1 Å showed the highly impressive removal of the heavy compounds, especially aromatic hydrocarbons. This is because Al-MCM-41 has a smaller pore size of 33.1 Å, which better fits with the size of aromatic compounds in oil (8-16 Å by average), than Al-SBA-15, driving higher sticking possibility on the active sites and then higher reactivity. Moreover, Al-MCM-41 did not only enhance petrochemical productivity, but also dramatically reduced sulfur content in oil products.

5.2 Introduction

Tire-derived oil seems to be the attractive product from tire pyrolysis because it can be used as a feed to produce gasoline, kerosene, etc. Furthermore, the petrochemicals (benzene, toluene, ethylbenzene, mixed-xylenes, styrene, etc.) can be also obtained from this oil. Thus, pyrolysis is one of the effective processes for end-life tire removal. However, the oil cannot be directly used as fuel due to a high concentration of aromatic compounds and hetero-atoms. According to Pithakratanayothin and Jitkarnka (2014), the chemical components in maltene solution, analyzed using GCxGC/TOF-MS, were classified into 8 groups based on their structures; that are, saturated hydrocarbon (SATs), olefins (OLEs), naphthenes (NAPs), terpenes (TERs), mono-aromatics (MAHs), poly-aromatics (PAHs) and polar-aromatics (PPAHs). The improvement of oil qualities was the important issue because 60-65 % heavy fractions (gas oil, light and heavy vacuum gas oils) and especially 20-25 % large-size aromatics (DAHs, PAHs, and PPAHs) still remained in tire-derived oil from thermal pyrolysis (Yuwapornpanit and Jitkarnka, 2015). After that, Seng-eiad and Jitkarnka (2015) estimated the average molecular kinetic and maximum sizes of hydrocarbon groups in TDO, and found that approximately 63.1 % of large-size hydrocarbons (> 8 Å) was distributed in TDO, which were mainly composed of 45.6 % aromatics (MAHs, DAHs, PPAHs, and PPAHs), together with 12.5 % aliphatics (SATs and OLEs) and 5.0 % alicyclics (NAPs and TERs). Most of them are in gas oil, light vacuum gas oil, and heavy vacuum gas oil fractions, especially PAHs followed by PPAHs, MAHs, and DAHs. Furthermore, their average maximum diameter ($Ø_{m.avg}$) were mostly in the range of 8-16 Å. Thus, large-pore size catalysts (pore size 20-30 nm) were suggested for reducing these bulky compounds.

Since C-H bond (88.5 kcal/mol) is weaker than C-C bond (102 kcal/mol); thus, hydrogen from thermal cracking can be highly produced (Malvin and Poutsma, 2000; Shi and Que, 2003). The incensement of hydrogenation, dehydrogenation, and ring-opening reaction can be provided by the functional of an active metal (Dũng *et al.*, 2009). However, the main reaction in pyrolysis of waste tire via thermal decomposition and catalytic reaction is β-scission, favored at β position in a

hydrocarbon molecule (Choi *et al.*, 2000; Chen *et al.*, 2002). Jin *et al.* (2012) found that MCM-41 gave a high catalytic activity and good selectivity to styrene monomer in the catalytic cracking of polystyrene. The side reaction yielded ethylbenzene, isopropylbenzene, isopropenylbenzene, and a secondary cross-linking product. In 2009, Dũng *et al.* stated that Ru/MCM-41 can be used to enhance naphtha and kerosene fractions, resulted from a high conversion of poly- and polar-aromatics. Moreover, alkylation was favored when Ru/MCM-41 was used. Ajaikumar *et al.* (2013) proposed that α-pinene was converted to 49.1 wt% mono-aromatics, tricyclene, camphene, terpinolene and limonene by using SBA-15. It is because the functional group of silanol on SBA-15 surface can exchange ions with both organic and inorganic compounds, causing the molecular reformation (Cesarino *et al.*, 2007).

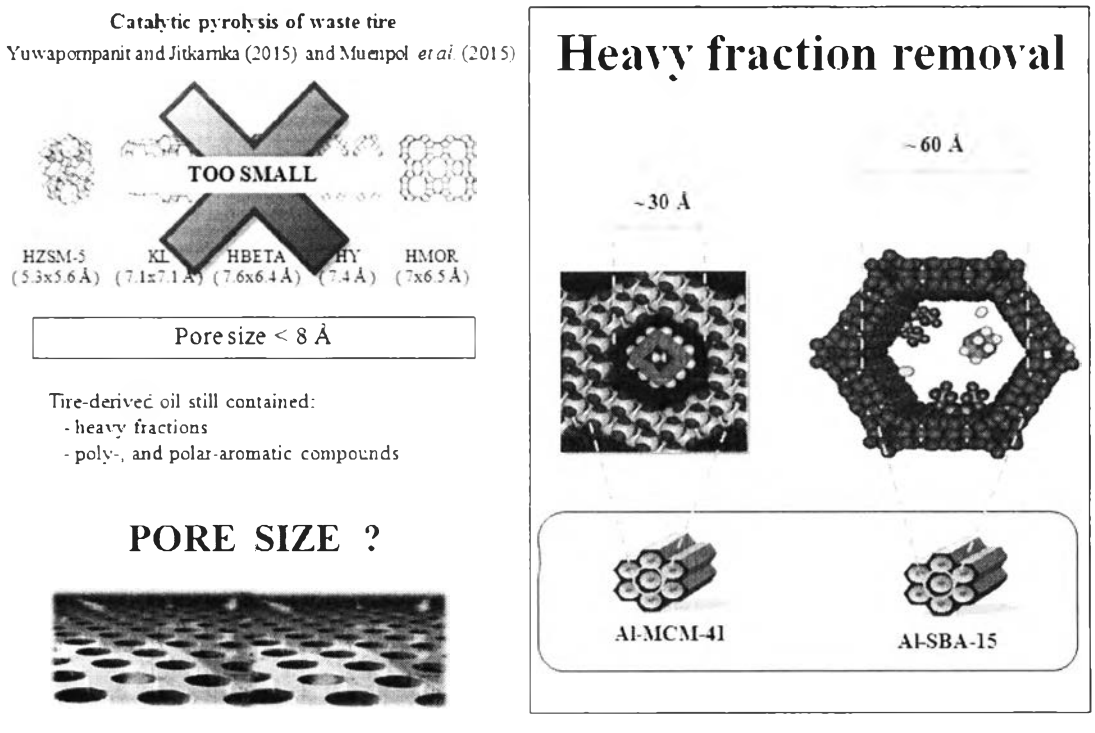

Figure 5.1 Determination of suitable pore size of mesoporous catalysts for removal of poly- and polar-aromatics in TDOs.

Since the large-size hydrocarbons were mainly aromatic compounds mostly distributed in gas oil fractions, and their average maximum diameter ($Ø_{m,avg}$) were in the range of 8-16 Å (Seng-eiad and Jitkarnka, 2015); thus, commercial Al-MCM-41 (pore size ~ 30 Å) and Al-SBA-15 (pore size ~ 60 Å) with the hexagonal structure and acid density were selected in this work. The aims of this work were therefore to study the effect of mesoporous Al-MCM-41 and Al-SBA-15 with two different pore sizes on the conversion of heavy fractions in waste-tire derived oil into lighter oil products. Moreover, since the pore size of zeolites have been found too small to adequately remove heavy PAHs and PPAHs molecules in TDO (Muenpol and Jitkarnka, 2015), the suitable pore size was also determined (see Figure 5.1) from the estimated molecular size distribution of all hydrocarbon groups. A catalyst with the suitable pore size was expected to have a high potential on the enhancement of light products. The analysis on aromatic compounds was carried out based on their molecular size distribution. Furthermore, petrochemical productivity and hetero-atom removal were also determined in this work.

5.3 Experimental

5.3.1 Catalyst Preparation

Mesoporous Al-MCM-41(~ 30 Å) and Al-SBA-15 (~ 60 Å) materials (Figure 5.1) were supplied by Green Stone Swiss Co., Limited (Shanghai, China). They were calcined at 540 °C for 6 h with the heating rate of 2 °C/min, subsequently pelletized, and sieved to obtain a particle size in the range of 40-60 mesh prior to their utilization.

5.3.2 Catalyst Characterization

The small-angled x-ray diffraction (XRD) patterns were obtained to confirm the hexagonal structure of Al-MCM-41 and Al-SBA-15. The diffractograms were recorded on a Riguku D/Max2200H apparatus with 50 kW, 300 mA Cu anode in a long fine focus ceramic X-ray tube for generating a CuKα radiation (1.5405 Å) with the scanning speed of 2 °/min and 2θ from 0.4° to 7°. Field Emission-Scanning Electron Microscope (FE-SEM), Hitachi Model S4800, was utilized to identify the

morphology of mesoporous materials. The x-ray fluorescence (XRF) spectrometry (AXIOS PW4400) was used to determine the percentage of Si and Al containing in mesoporous materials. The powder samples were hydraulically pressed to give a flat surface with the sample to boric acid mass ratio of 1:3. The nitrogen adsorption–desorption experiment using ThermoFinnigan/Sorptomatic1990 instrument was performed to determine specific surface area, pore volume and average pore diameter of the mesoporous materials. The specific surface area was determined using BET method. The average pore diameter and the pore size distribution were calculated through the BJH method. Approximate 0.1 g of sample was degassed at 250 °C for 12 h prior to analysis. In addition, Thermogravimetric/Differential Thermal Analysis (TG/DTA) was used to determine the deposition of coke on spent catalysts. The temperature was ramped from 30 °C to 900 °C with the heating rate of 10 °C/min under 20 mL/min oxygen.

5.3.3 Pyrolysis of Waste Tire

The pyrolysis reactor was divided into 2 zones, as the same system in Yuwapornpanit and Jitkarnka (2015). The upper zone was the catalytic zone (350 °C), and the lower zone was the pyrolytic zone (500 °C). Waste automobile tire (Bridgestone TURANZA GR-80) was first scraped, and then sieved to obtain the small particle size in the range of 20-40 mesh. Firstly, 30 g of the waste tire sample was loaded into the lower zone, and 7.5 g of catalyst granules was loaded into the catalytic zone. Then, tire sample was heated with heating rate of 10 °C/min from room temperature to 500 °C under 30 ml/min nitrogen pressure, and subsequently held for 120 min at the final temperature. The gas products were carried out to two condensers for condensing the liquid product, and the other incondensable gas was collected in the sampling gas bag.

5.3.4 Products Analysis

The contents of carbon, hydrogen, nitrogen, and sulfur in liquid products were acquired from using LECO®Elemetal Analyzer (TruSpec®S). The gas compositions were detected using a Gas Chromatography (GC-FID), Agilent Technologies 6890 Network GC system (HP-PLOT Q column: 20 μm film thickness

and 30 m × 0.32 mm ID). The liquid products were firstly dissolved in *n*-pentane in the oil/*n*-pentane mass ratio of 40:1 for precipitating asphaltene. After that the asphaltene was filtered using polyamide membrane (pore size: 0.45μm). The obtained liquid is called maltene. The 30 μL maltene was diluted in 2 mL carbon disulfide (CS_2) prior to analyze with GC instruments. The true boiling point curve were determined using a Varian GC-3800 simulated distillation gas chromatograph (SIMDIST-GC) conformed to the ASTM-D2887 method. The instrument equipped with FID and WCOT fused silica capillary column (15 m × 0.25 mm ID × 0.25 μm film thichness). The true boiling point curves were cut into petroleum fractions according to their boiling points; gasoline (< 149 °C), kerosene (149-232 °C), gas oil (232-343 °C), light vacuum gas oil (343-371 °C) and heavy vacuum gas oil (> 371 °C). Finally, the chemical composition of maltene solution was determined using a comprehensive two-dimensional Gas Chromatography with Time of Flight Mass Spectrometer (GC×GC/TOF-MS). The GC×GC/TOF-MS apparatus, equipped with an Agilent gas chromatograph 7890 (Agilent Technologies, Palo Alto, CA, USA), a Pegasus® 4D TOF/MS (LECO, St. Joseph, MI, USA) and a thermal modulator, was used to analyze oil compositions. The instrument was operated by the cooperation of two GC columns. The 1st GC column was a non-polar Rtx®-5Sil MS and the 2nd GC column was a polar Rxi®-17 MS. Total Ion Chromatograms (TICs) of maltenes obtained from GCxGC/TOF-MS were plotted in forms of 2D (Contour Plots) and 3D (Surface Plots) in order to observe the distribution of hydrocarbon groups in the chromatograms. The external standard (PIANO, Spectrum Quality Standards, Ltd.) containing benzene (2.425 wt%), toluene (2.576 wt%), ethylbenzene (2.504 wt%), p-xylene (3.374 wt%), and cumene (1.864 wt%) was used for calibrating the peaks of petrochemical products (BTEXC). The PIANO standard was firstly diluted in CS_2 in the PIANO standard/CS_2 volume ratio of 1:10 and then the 30 μL diluted standard was further diluted in 2 mL CS_2 prior to analysis with GCxGC/TOF-MS instruments.

5.3.5 Determination of Average Maximum Diameters of Molecules in TDOs

According to Israel (2013), the sampling size (n) of hydrocarbon in each molecular group was determined using Yamane method as seen in Eq. (5.1), where N is the population of hydrocarbons in each group, and a ninety percent confidence level was assumed for this equation (e = 0.1).

$$n = \frac{N}{1 + N(e)^2} \tag{5.1}$$

Then, the maximum diameters of the sampling compounds were estimated using the published data from ChemSpider (Royal Society of Chemistry, 2015). Finally, the average maximum diameter in each distribution range was calculated using Eq. (5.2), where ω and m are defined as the weight fraction of each species and the number of species in each range, respectively.

$$\emptyset_{avg} = \frac{\sum_{i=1}^{m} \omega_i \emptyset_i}{\sum_{i=1}^{m} \omega_i} \tag{5.2}$$

5.4 Results and Discussion

5.4.1 Catalyst Characterization

The SAXS patterns of commercial Al-MCM-41 and Al-SBA-15 are displayed in Figure 5.2a. The crytallinity of mesoporous materials is assured by the first diffraction peaks corresponding to the (100) planes (Gobara, 2012) of both Al-MCM-41 and Al-SBA-15 that occur at 2Θ = 1.870° and 0.4°, respectively. Obviously, it can be observed that the peaks at (100) plans of Al-MCM-41 and Al-SBA-15 appear at a low two-theta, exhibiting the large pore materials. Figures 5.2b1 and 5.2b2 show FE-SEM micrographs of Al-MCM-41 and Al-SBA-15, exhibiting

that the molecular sieves have the similar morphology. However, Al-MCM-41 has larger cluster sizes than Al-SBA-15. The characteristic IV isotherm of Al-MCM-41 presents sharp steps at intermediate pressures corresponding to the capillary steps of mesoporous structure (Lin *et al.*, 2014) whereas that of Al-SBA-15 presents large hysteresis loop, exhibiting wide and large pore distribution as seen in Figure 5.2c.

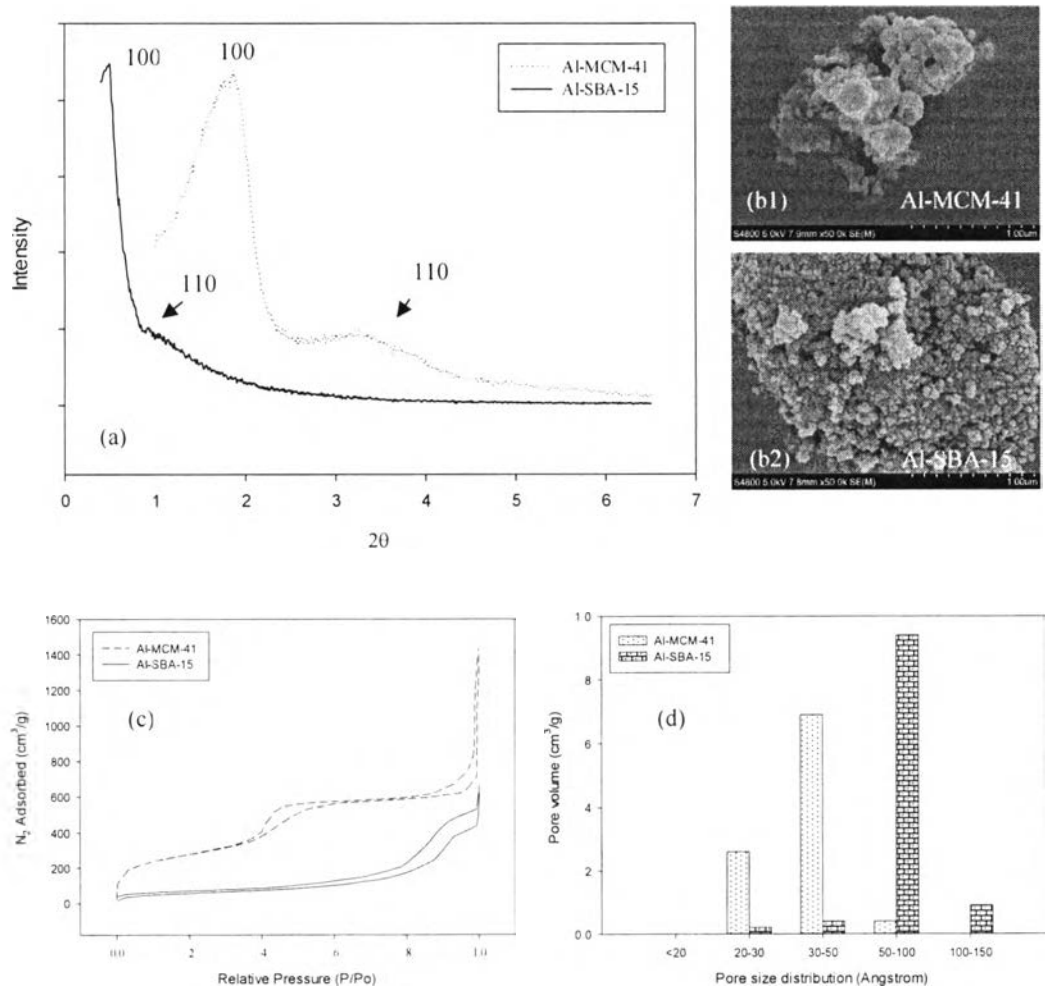

Figure 5.2 (a) SAXS patterns, (b) FE-SEM image, (c) isotherms, and (d) pore size distributions of Al-MCM-41 and Al-SBA-15.

The properties of the fresh catalysts analyzed using N_2 adsorption-desorption are summarized in Table 5.1. The unit cell of hexagonal of Al-MCM-41 and Al-SBA-15 can be calculated by using the equation; $a_0 = 2d_{100}/\sqrt{3}$, where d spacing belongs to the (100) plane. Al-SBA-15 with the large pore size of 60.5 Å has

a lower surface area than Al-MCM-41 (33.1 Å). The amount of Si in Al-MCM-41 material is similar to that in Al-SBA-15 material, indicating that Al-MCM-41 and Al-SBA-15 have the similar acid density.

Table 5.1 Porous properties of mesoporous Al-MCM-41 and Al-SBA-15

Mesoporous Materials	d_{100}[a] (Å)	a_o[a] (Å)	BJH Pore Diameter (Å)	Specific Pore Volume (cm^2/g)	S_{BET} (m^2/g)	$\frac{Si^c x100}{Si + Al}$ (%)
Al-MCM-41	47.2	54.5	33.1	0.83	993	98.73
Al-SBA-15	95.9	110.8	60.5	0.77	205	98.82

[a] d_{100} spacing of Al-MCM-41 and Al-SBA-15 presenting at plane (100)
[b] Unit cell (a_o) = $2d_{100}/\sqrt{3}$ for hexagonal structure
[c] XRF

5.4.2 Products from Waste Tire Pyrolysis

The distribution of products indicates that Al-MCM-41 and Al-SBA-15 do not result in significant increases in gas and liquid products, because a high amount of coke is generated using the mesoporous catalysts. However, Al-MCM-41 can promote coke formation on the catalyst surface more highly than Al-SBA-15, indicating that surface activity of Al-MCM-41 is higher than Al-SBA-15.

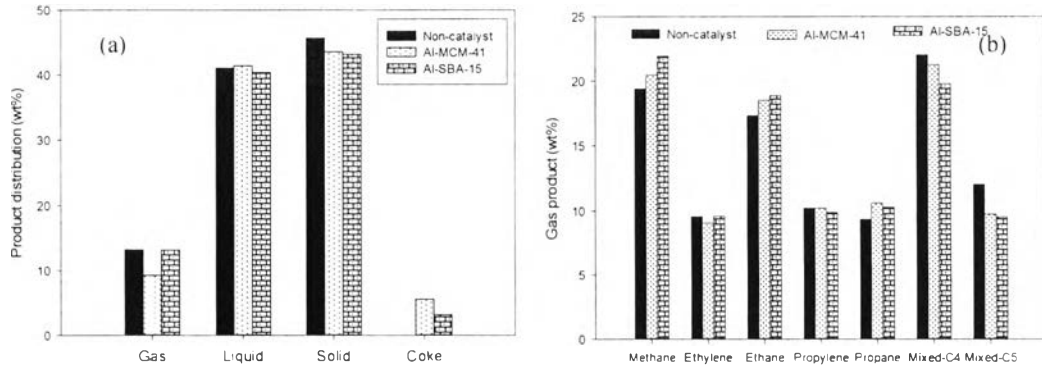

Figure 5.3 (a) Product distributions and (b) gas products from using Al-MCM-41 and Al-SBA-15.

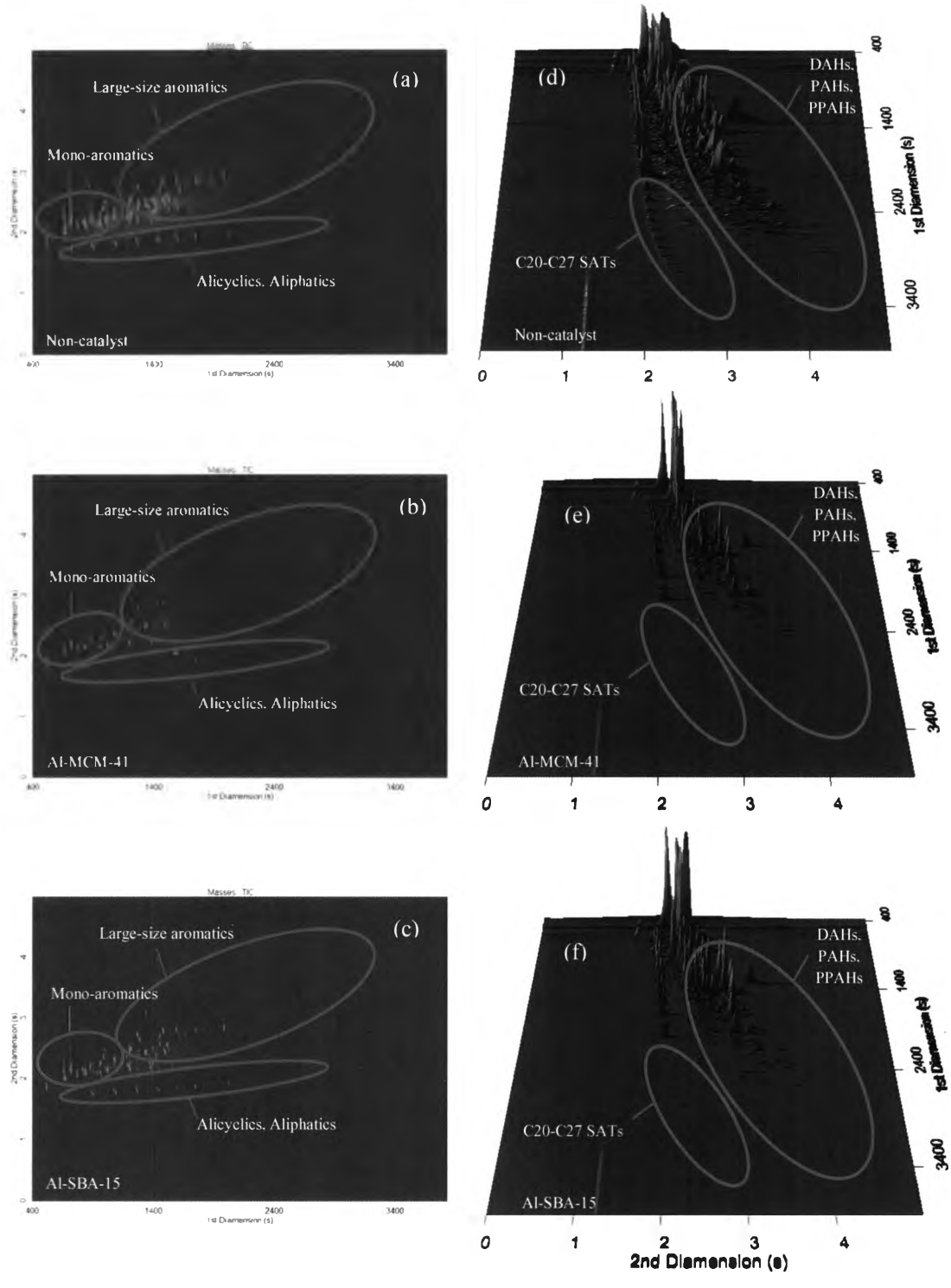

Figure 5.4 Total Ion Chromatograms of maltenes: contour plots (2D) in cases of (a) non-catalyst, (b) Al-MCM-41, and (c) Al-SBA-15, and surface plots (3D) in cases of (d) non-catalyst, (e) Al-MCM-41, and (f) Al-SBA-15.

Figure 5.4 illustrates the contour and surface plots of Total Ion Chromatogram (TIC) of maltenes from using Al-MCM-41 and Al-SBA-15. According to the IUPAC, the hydrocarbon species can be classified into three main categories; that are, aliphatics, alicyclics, and aromatics as located in Figures 5.4a-5.4c. Aliphatics are classified into two classes; that are, SATs and OLEs. Alicyclics are classified into two classes; that are, NAPs and TERs. Aromatics are classified into four classes; that are, MAHs, DAHs, PAHs, and PPAHs. All the chemical groups in maltene solutions are displayed in Figure 5.5a. It can be observed that Al-MCM-41 and Al-SBA-15 can highly suppress the formation of DAHs, PAHs, and PPAHs, especially C20-C27 SATs, whereas the other groups are increased which can obviously observed in Figures 5.4e-5.4f. It can be inferred that the reduction of DAHs, PAHs, and PPAHs causes the enhancement of OLEs, NAPs, and TERs, especially MAHs via ring opening (Du *et al.*, 2005) possibly. Furthermore, the decrement of C/H ratio of tire-derived oil with using Al-MCM-41 and Al-SBA-15 in Table 5.2 indicates that these molecular sieves can promote hydrogenation of aromatics, forming TERs and NAPs, and can also enhance hydrogenation of OLEs, forming SATs. Moreover, Al-MCM-41 produces MAHs and PAHs more highly than Al-SBA-15, resulted from dehydrogenation and aromatization of OLEs, NAPs, and TERs (Meng *et al.*, 2013; Kwak *et al.*, 2014) since the decreases of these compounds are greater than those occurring on Al-SBA-15.

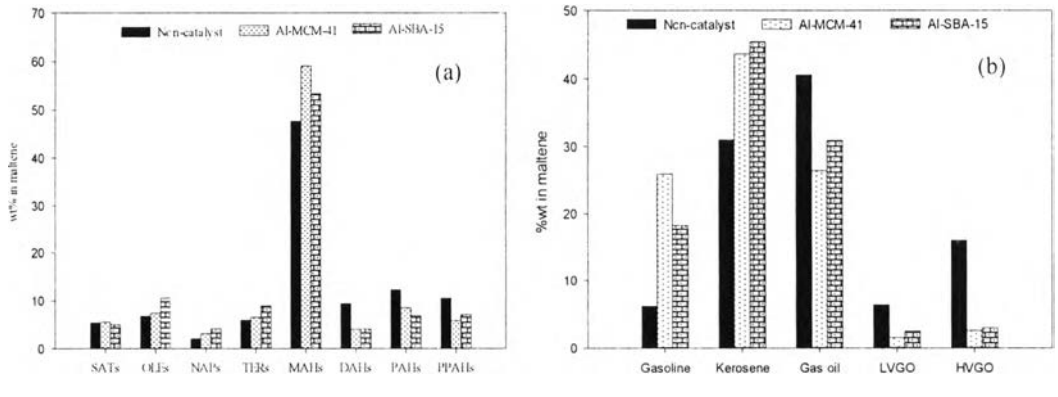

Figure 5.5 (a) Chemical compositions and (b) petroleum fractions from using Al-MCM-41 and Al-SBA-15.

Table 5.2 Ultimate analysis of tire-derived oils

Ultimate Analysis (wt%)	C	H	C/H ratio
Non-catalyst	69.10±0.42	9.62±0.15	7.19
Al-MCM-41	61.70±0.85	9.46±0.21	6.53
Al-SBA-15	66.25±1.63	9.84±0.04	6.73

The petroleum fractions of Al-MCM-41 and Al-SBA-15 cases are displayed in Figure 5.5b. Both Al-MCM-41 and Al-SBA-15 dramatically decrease heavy fractions (LVGO, and HVGO) in oils by 81.6 % and 75.7 %, respectively. Also, gas oil is reduced using both molecular sieves by 34.9 % and 23.8 %, respectively, which therefore drastically enhances gasoline content by approximately four times for Al-MCM-41 case and three times for Al-SBA-15 case, and increases kerosene content by 40.7 % for Al-MCM-41 and 46.59 % for Al-SBA-15. As a result, it can be included that the large porosity of Al-MCM-41 and Al-SBA-15 can contribute to the diffusion of bulky molecules into the pore where a large number of active sites are. It may enhance the inner pore reaction, catalyzing the larger molecular into the smaller molecules (Cao *et al.*, 2009). However, Al-MCM-41 is likely to perform on catalytic cracking better than the Al-SBA-15 since it more greatly converts gas oil, resulting in the lighter liquid product. It can be explained that Al-MCM-41 has a smaller pore size of 33.1 Å, which is better fit with the average maximum size of large aromatic compounds in oil (8-16 Å by average), than Al-SBA-15, driving higher sticking possibility on the active sites, and then higher reactivity.

5.4.3 Molecular Size Distribution of Aromatic Compounds in Tire-derived Oils

Seng-eiad and Jitkarnka (2015) found that using the average kinetic diameter ($Ø_{k,avg}$) in catalyst design for pyrolysis of waste tire may not be suitable because the $Ø_{k,avg}$ obtained from the calculation is in the range of 6.6-8.1 Å; therefore, some catalysts with this range of pore size, like HBETA, HY, and HMOR, should have been able to handle the heavy fractions, but they could not have (Yuwapornpanit and Jitkarnka, 2015). Therefore, the average maximum diameter

($Ø_{m,avg}$) of compounds, which is defined as the longest part of molecule, in TDOs must be acquired. Therefore, in this work, the estimation of $Ø_{m,avg}$ of compounds in TDOs obtained from both mesoporous catalysts was next performed as follows.

Table 5.3 Sampling size and representatives from each molecular group of compounds

Molecular Group	Number of Detected Compounds			Number of Sampling Size[a]			%Area of Detected Compounds			%Area of Sampling		
	1	2	3	1	2	3	1	2	3	1	2	3
SATs	42	55	61	30	35	38	5.3	5.5	5.0	5.2	5.4	4.8
OLEs	110	106	129	52	51	56	7.4	7.4	10.5	6.2	6.5	9.6
NAPs	42	64	96	30	39	49	2.0	3.2	4.1	1.9	3.0	3.8
TERs	100	109	143	50	52	59	6.7	6.5	8.9	5.8	5.7	7.5
MAHs	231	203	240	70	67	71	46.9	59.1	53.5	40.6	50.0	45.9
DAHs	27	16	25	21	14	20	9.2	4.0	4.1	9.2	4.0	4.1
PAHs	96	72	93	49	42	48	12.1	8.5	6.9	11.2	8.0	6.5
PPAHs	174	141	193	64	59	66	10.4	5.7	7.1	9.0	5.2	6.3
Total	822	766	980	365	359	407	100	100	100	89.0	87.7	88.4

[a]Yamane method (Israel, 2013), 1 = Non-catalyst, 2 = Al-MCM-41, 3 = Al-SBA-15

The number of representatives of each molecular group was first determined from Yamane method (Israel, 2013) as shown in Table 5.3. Out of more than 750 species that are normally detected in TDOs, the sampling size is in the range of 359-407 species, accounting for 87.7-89.0 % of total sampling area. Moreover, the area percentage of samples in each group shows that the sampling was well handled. Then, the average maximum diameters of all hydrocarbon groups were calculated, and the molecular size distributions were plotted and shown in Figure 5.6. The molecular sizes of some dominant aromatic compounds are shown in Table 5.4.

Table 5.4 Molecular size of dominant aromatic compounds in TDOs from using Al-MCM-41 and Al-SBA-15

Chemical Name	Exact Mass (m/z)	Maximum Diameter (O_m, Å)[a]	% Area[b]		
			1	2	3
Mono-aromatics (MAHs)					
Benzene	78.0469	4.86	-	-	-
Toluene	92.0626	5.85	-	1.80	0.56
Ethylbenzene	106.0782	7.09	1.50	4.57	3.30
mixed-Xylenes	106.0782	6.76-6.77	0.19	1.37	0.78
Styrene	104.0626	7.11	0.52	0.09	0.75
Cumene	120.0939	7.26	0.18	2.28	1.39
2,3-dihydro-1,6-dimethyl-1H-Indene	146.1095	7.78	1.42	1.36	1.05
Cyclopentyl-Benzene	146.1095	8.44	1.40	1.23	1.57
Pentyl-Benzene	148.1252	10.66	1.34	1.05	0.86
1-heptenyl-Benzene	174.1408	12.85	0.53	0.59	0.56
Octyl-Benzene	190.1721	14.44	0.28	0.15	0.16
Di-aromatics (DAHs)					
1-ethyl-Naphthalene	156.0939	7.55	0.79	0.53	0.85
1,4,5-trimethyl-Naphthalene	170.1095	8.17	0.63	0.41	0.55
1-methyl-7-(1-methylethyl)-Naphthalene	184.1252	9.31	0.14	0.11	0.08
2-butyl-Naphthalene	184.1252	11.58	0.07	0.03	-
1-hexyl-Naphthalene	212.1565	12.26	0.02	-	-
Poly-aromatics (PAHs)					
Biphenyl	154.0782	9.28	1.60	0.83	0.80
4-methyl-1,1'-Biphenyl	168.0939	10.23	1.73	1.13	0.92
4-Ethylbiphenyl	182.1095	11.43	0.38	0.29	0.20
1,1'-(1,3-propanediyl)bis-Benzene	196.1252	11.74	1.32	0.92	0.63
1,1'-(1,4-butanediyl)bis-Benzene	210.1408	13.73	0.25	0.18	0.16
Polar-aromatics (PPAHs)					
Aniline	93.0578	5.69	0.57	0.04	0.04
Benzothiazole	135.0142	6.71	2.44	0.78	0.99
2,5-diethyl-Thiophene	140.0659	8.48	0.15	0.01	0.14
(+-)-N-Benzyl-alpha-methyl-N-nitrosobenzylamine	240.1262	11.69	0.17	-	0.01
8-Phenyl-1-octanol	206.1670	15.43	0.32	0.28	0.14

[a]Royal Society of Chemistry (2015), [b]GCxGC/TOF-MS, 1 = non-catalyst, 2 = Al-MCM-41, and 3 = Al-SBA-15

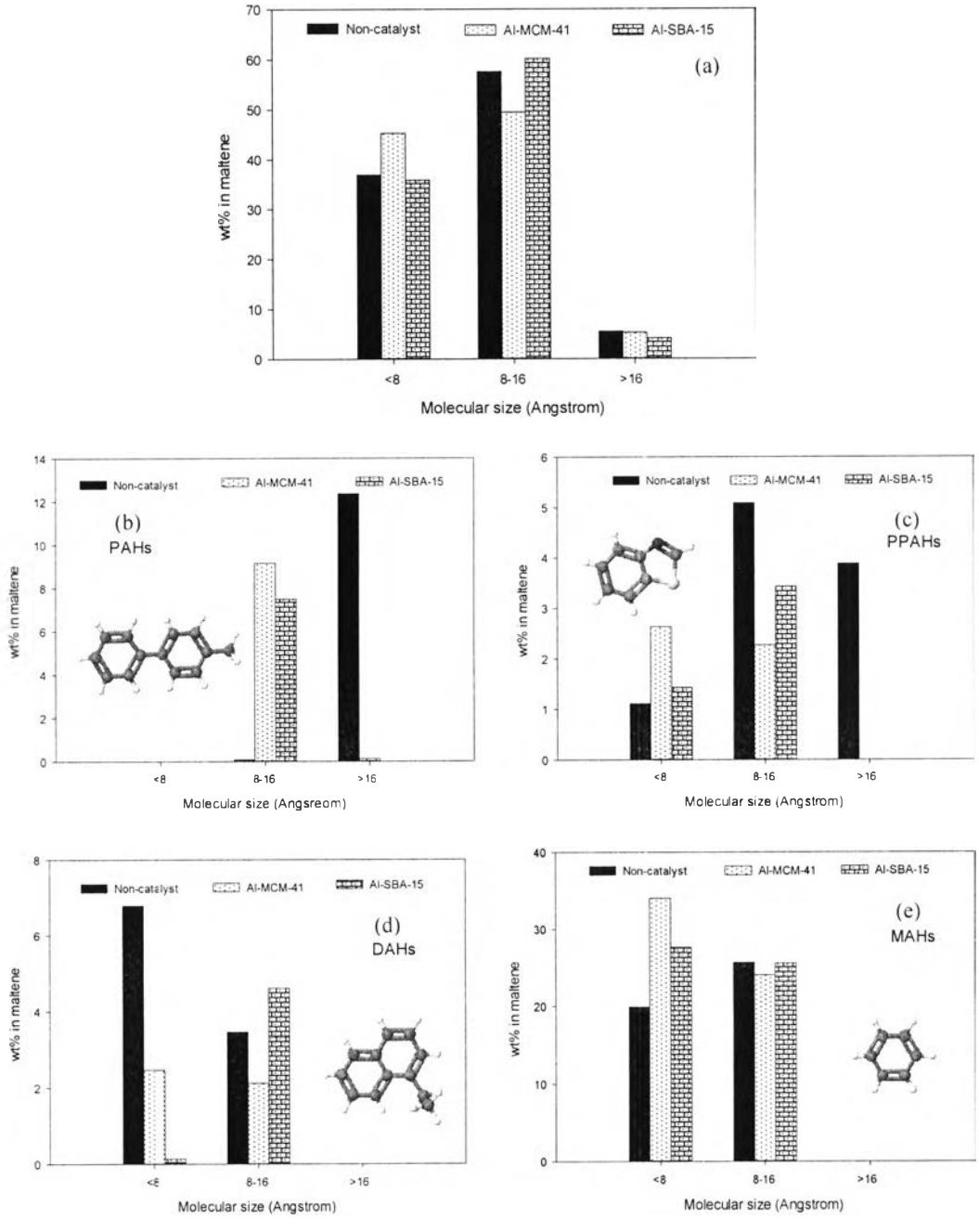

Figure 5.6 Molecular size distribution: (a) all groups, (b) polar-aromatics (PPAHs), (c) poly-aromatics (PAHs), (d) di-aromatics (DAHs), and (e) mono-aromatics (MAHs) in maltene obtained from using Al-MCM-41 and Al-SBA-15.

The maximum diameters, $Ø_m$, in all cases are found distributed in tri-modal distribution. Therefore, the average maximum diameters, $Ø_{m,avg}$, were calculated into 3 ranges of sizes; that are, small (< 8 Å), medium (8-16 Å), and large sizes (> 16 Å) as seen in Figures 5.6a-5.6e. It has been noticed in Figure 5.3c that the TDOs from using Al-MCM-41 and Al-SBA-15 still mainly contain aromatics; however, Al-MCM-41 and Al-SBA-15 can dramatically reduce DAHs, PAHs, and PPAHs. Interestingly, Figure 5.6a indicates that Al-MCM-41 more greatly decreases the medium-size (8-16 Å) molecular concentration of all hydrocarbon groups whereas Al-SBA-15 would rather reduce the concentration of large-size molecules (> 16 Å). It indicates that Al-MCM-41 pore (33.1 Å) better fits with the medium-size (8-16 Å) molecular feed than Al-SBA-15; however, Al-SBA-15 pore (60.5 Å) greater fits to the large-size molecules (> 16 Å). Figure 5.6b shows the molecular size distributions of poly-aromatics. The result shows that the large size poly-aromatics (> 16 Å) are extremely reduced by using Al-MCM-41 and Al-SBA-15 via cracking, resulting the increase of the medium-size poly-aromatics (8-16 Å). Figure 5.6c displays the molecular size distribution of polar-aromatics. It can be observed that Al-MCM-41 and Al-SBA-15 completely crack the large size polar-aromatics (> 16 Å), and also extremely crack the medium size polar-aromatics (8-16 Å) into the small size polar-aromatics (< 8 Å). From poly- and polar aromatic size distributions, it can be concluded that the mesoporous catalysts with the pore sizes of 33.1-60.5 Å can provide the almost complete cracking of these large-size molecules in tire-derived oils.

Figure 5.6d presents the molecular size distribution of di-aromatics. The result indicates that Al-MCM-41 and Al-SBA-15 drastically decrease the di-aromatics with small sizes (< 8 Å). Moreover, the medium-size di-aromatics (8-16 Å) are drastically reduced using Al-MCM-41 whereas it is increased in Al-SBA-15 case. According to the results, it can be implied that the decrement of the small size di-aromatics results in the increments of mono-aromatics and non-aromatics. Figure 5.6e exhibits the molecular size distribution of mono-aromatics. As a results, Al-MCM-41 slightly decreases the medium size mono-aromatics (8-16 Å) whereas in the case of Al-SBA-15, the medium size mono-aromatics is still unchanged. Interestingly, both Al-MCM-41 and Al-SBA-15 catalysts considerably increase the

mono-aromatics with small sizes (< 8 Å), which are mostly referred to petrochemical products as reported in Table 5.4. Therefore, the enhancement of small size mono-aromatic concentration can possibly be mainly caused by the reduction of di-, poly-, and polar-aromatics. In addition, the Al-MCM-41 catalyst with the pore size of 33.1 Å can more greatly enhance mono-aromatic formation than the Al-SBA-15 catalyst. Thus, in the next section, the petrochemical productivity was calculated, and discussed.

5.4.4 Petrochemical Productivity using Mesoporous Al-MCM-41 and Al-SBA-15

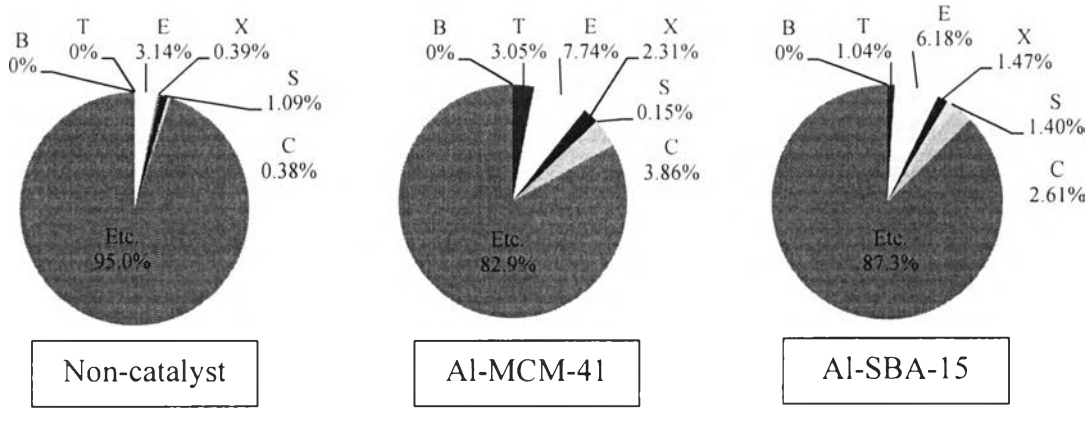

Figure 5.7 Percentage of petrochemicals in mono-aromatics (B = Benzene, T = Toluene, E = Ethylbenzene, X = Mixed-xylenes, S = Styrene, and C = Cumene).

The percentage of petrochemicals in mono-aromatics is shown in Figure 5.7. Interestingly, both Al-MCM-41 and Al-SBA-15 can enhance the production of petrochemicals in mono-aromatic fraction. The thermal pyrolysis gives 5.0 % petrochemicals in mono-aromatics whereas Al-MCM-41 and Al-SBA-15 give 17.1 % and 12.7 %, respectively. Moreover, Al-MCM-41 produces a higher content of toluene, ethylbenzene, mixed-xylenes, and cumene than Al-SBA-15. In addition, Al-MCM-41 gives remarkably the highest overall petrochemical productivity as reported in Table 5.5.

Table 5.5 Petrochemical productivity using Al-MCM-41 and Al-SBA-15 in waste tire pyrolysis

Catalyst	Petrochemical Productivity (kg/ton of tire)
Non-catalyst	9.8
Al-MCM-41	41.2
Al-SBA-15	29.3

From the results, it is clearly seen that Al-MCM-41, which has higher surface area and its pore size that better fits with molecules in the feed than Al-SBA-15, can convert large-size aromatics to petrochemical products more greatly than Al-SBA-15. Furthermore, the highest increment of ethylbenzene may be resulted from the hydrogenation of styrene because styrene is highly reduced when Al-MCM-41 is introduced. Then, ethylbenzene may be further converted, forming cumene, toluene, and mixed-xylenes via free radicals. However, the concentration of benzene in maltene solution is extremely lower than that of ethylbenzene. It indicates that the benzene radical might react with a hydrocarbon to form another compound.

5.4.5 Hetero-atom Removal using Mesoporous Al-MCM-41 and Al-SBA-15

Table 5.6 Ultimate analysis of hetero-atom (S,N) contents in tire-derived oils

Ultimate Analysis (wt%)	S	N
Non-catalyst	1.27±0.00	0.40±0.04
Al-MCM-41	0.88±0.00	0.52±0.04
Al-SBA-15	0.88±0.00	0.55±0.04

Al-MCM-41 and Al-SBA-15 can reduce sulfur from 1.27 wt% to 0.88 wt% whereas nitrogen content increases from 0.40 % to around 0.5 % as seen in Table 5.5. Moreover, sulfur contents in oils from using both mesoporous catalysts are not different as seen in Table 5.5. It indicates that Al-MCM-41 can convert sulfur compounds in aromatic fraction to another compound via cracking reaction and

hydrogenation better than Al-SBA-15. On the other hand, both Al-MCM-41 and Al-SBA-15 cannot reduce nitrogen content in oil.

5.5 Conclusions

Since the average maximum diameter of molecules in tire-derived oil were found mainly distributed in the range of 8-16 Å, commercial Al-MCM-41 (pore size = 33.1 Å) and Al-SBA-15 (pore size = 60.5 Å) with the similar hexagonal structure and acid density were selected in this work for studying the effect of pore size in removal of heavy fractions (gas oil, light and heavy gas oils), especially large-size aromatic compounds (> 16 Å). The results indicated that the mesoporous catalysts with pore sizes of 33.1 and 60.5 Å can result in the almost complete cracking of large size poly- and polar-aromatics in tire-derived oils. However, the Al-MCM-41 with the pore size of 33.1 Å exhibited more impressive reduction of heavy fractions (gas oil, LVGO, and HVGO) and large-size aromatics (DAHs, PAHs, and PPAHs) with sizes > 16 Å than the Al-SBA-15 with the pore size of 60.5 Å. Thus, it is recommended that a mesoporous catalyst with the pore size of around 30 Å be appropriate for removal of large-size aromatics (> 16 Å) and consequent reduction of heavy fractions in TDO. Too large pore size of a mesoporous catalyst prevents molecules from accessing to the active sites. Moreover, the Al-MCM-41 catalyst was better, not only in removing those heavy compounds but also in producing the higher quantity of petrochemicals. Additionally, even though Al-MCM-41 and Al-SBA-15 cannot reduce nitrogen content in oil, they can greatly remove sulfur in oil (approximately 1.4 times).

5.6 Acknowledgements

The authors would like to thank The Petroleum and Petrochemical College, Chulalongkorn University, Thailand, Center of Excellence on Petrochemical and Materials Technology, and Thailand Research Fund (TRF: RSA5680021) for all supports.

5.7 References

Ajaikumar, S., Golets, M., Larsson, L., Shchukarev, S., Kordas, K., Leino, A.R., and Mikkola, J.P. (2013) Effective dispersion of Au and Au–M (M = Co, Ni, Cu and Zn) bimetallic nanoparticles over TiO2 grafted SBA-15: Their catalytic activity on dehydroisomerization of a-pinene. Microporous and Mesoporous Materials, 173, 99–111.

Cao, Q., Jin, L., Bao, W., and Lv., Y. (2009) Investigations into the characteristics of oils produced from co-pyrolysis of biomass and tire. Fuel Processing Technology, 90, 337-342.

Cesarino, I., Marino, G., Matos, J.D.R., and Cavalheiro, E.T.G. (2007) Using the organofunctionalised SBA-15 nanostructured silica as a carbon paste electrode modifier: Determination of cadmium ions by differential anodic pulse stripping voltammetry. Journal of the Brazilian Chemical Society, 18(4), 810-817.

Chen, F. and Qian, J. (2002) Studies on the thermal degradation of cis-1,4-polyisoprene. Fuel, 81, 2071–2077.

Choi, S.S. (2000) Characterization of bound rubber of filled styrene–butadiene rubber compounds using pyrolysis-gas chromatography. Journal of Analytical and Applied Pyrolysis, 55, 161–170.

Du, H., Fairbridge, C., Yang, H., and Ring, Z. (2005) The chemistry of selective ring-opening catalysts. Applied Catalysis A: General, 294(1), 1-21.

Dũng, N.A., Klaewkla, R., Wongkasemjit, S., and Jitkarnka, S. (2009) Light olefins and light oil production from catalytic pyrolysis of waste tire. Journal of Analytical and Applied Pyrolysis, 86, 281–286.

Gobara, H.M. (2012) Characterization and catalytic activity of NiO/mesoporous aluminosilicate AlSBA-15 in conversion of some hydrocarbons. Egyptian Journal of Petroleum, 21, 1-10.

Israel, G.D. (2013) Determining Sample Size. Florida: University of Florida.

Jin, S., Cui, K., Guan, H., Yang, M., Liu, L., and Lan, C. (2012) Preparation of mesoporous MCM-41 from natural sepiolite and its catalytic activity of cracking waste polystyrene plastics. Applied Clay Science, 56, 1–6.

Kwak, K.Y., Kim, M.S., Lee. D.W., Cho, Y.H., Han, J., Kwon, T.S., and Lee, K.Y. (2014) Synthesis of cyclopentadiene trimer (tricyclopentadiene) over zeolites and Al-MCM-41: The effects of pore size and acidity. Fuel, 137, 203-236.

Lin, J., Zhao, B., Cao, Y., Xu, H., Ma, S., Guo, M., Qiao, D., and Cao, Y. (2014) Rationally designed Fe-MCM-41 by protein size to enhance lipase immobilization, catalytic efficiency and performance. Applied Catalysis A: General, 478, 175–185.

Marvin, L. and Poutama. (2000) Fundamental reactions of free radicals relevant. Journal of Analytical and Applied Pyrolysis, 54, 5-35.

Meng, X., Wang, Z., Zhang, R., Xu, C., Liu, Z., Wang, Y., and Guo, Q. (2013) Catalytic conversion of C_4 fraction for the production of light olefins and aromatics. Fuel Processing Technology, 116, 217-221.

Muenpol, S., Yuwapornpanit, R., and Jitkarnka, S. (2015) Valuable petrochemicals, petroleum fractions, and sulfur compounds in oils derived from waste tyre pyrolysis using five commercial zeolites as catalysts: impact of zeolite properties. Clean Technology Environment Policy, DOI 10.1007/s10098-015-0935-8.

Pithakratanayothin, S. and Jitkarnka, S. (2014) Comparison of Components in Oil Derived from Tyre Pyrolysis with and without KL Catalyst Using GC×GC/TOF-MS. Chemical Engineering Transaction, 39, 1261-1266.

Royal Society of Chemistry. "ChemSpider." 2015. 20 October 2014 <www.ChemSpider.com>

Seng-eiad, S. and Jitkarnka, S. (2015) Estimation of average kinetic and maximum diameters of hydrocarbon groups in tyre-derived oil for catalyst design purpose. Chemical Engineering Transaction. (in press)

Shi, B. and Que, G. (2003) Cracking and cracking selectivity of alkane and alkyl aromatics: effects of dispersed catalysis and hydrogen donors. American Chemical Society, 48(2), 631-633.

Yuwapornpanit, R. and Jitkarnka, S. (2015) Cu-doped catalysts and their impacts on tire-derived oil and sulfur removal. Journal of Analytical and Applied Pyrolysis, 111, 200-208.